Int. J. Heat Mass Transfer. Vol. 8, pp. 1319–1331. Pergamon Press 1965. Printed in Great Britain

NATURAL CONVECTION AT A THERMAL LEADING EDGE ON A VERTICAL WALL

MAX G. SCHERBERG

Thermo-Mechanics Research Laboratory, Office of Aerospace Research, United States Air Force, Wright-Patterson Air Force Base, Ohio.

(*Received* 5 *August* 1964 *and in revised for* 7 *January* 1965)

Abstract—The natural convection from a thermal leading edge region ($T_w/T_\infty = 1 + \tau_0 x^n$, $n > 1$) is determined and matched with the known solution immediately above this region. It is shown that in this region there is a downward conduction of heat near the wall which flows back into the wall just above the leading edge so that there is a region just above this point in which the heat transfer is reversed to the expected direction of heat flow. Comparisons in temperature and velocity distributions at the matched position of the solutions are given for several values of the exponent n.

NOMENCLATURE

$\rho(x, y)$,	boundary-layer density [lb/ft^3];
$T(x, y)$,	boundary-layer temperature [°R];
$\delta(x)$,	boundary-layer thickness [ft];
x, y,	vertical and horizontal coordinates respectively [ft];
x_1,	wall position at conduction reversal [ft];
X,	vertical coordinate in x_1 units;
$\bar{\delta}$,	boundary-layer thickness in x_1 units;
$U(x, y)$,	boundary-layer velocity [ft/s];
u, u_1,	velocity functions;
τ,	temperature function ($\tau_0 x^n$);
τ_1,	heat-transfer function;
P_{cr},	critical solution parameter;
Pr,	Prandtl number;
$G_{\bar{T}}$,	heat-transfer function;
K,	slope of boundary-layer edge at $x = 0$;
K_{s_2},	solution function for matching.

Subscripts

∞,	conditions at boundary-layer edge;
w,	conditions at wall;
mat,	condition at solution matching;
max,	maximum value;
LES,	leading edge solution;
US,	solution above leading edge region.

NATURAL CONVECTION AT A THERMAL LEADING EDGE ON A VERTICAL WALL

IN PAPERS [1], [2] which studied natural convection along a vertical wall near and above the thermal leading edge and along wall sections under several starting or initial conditions for flow speed and temperature distribution of the natural convection type, it became clear that the investigation could not be extended to a thermal leading edge unless the vertical heat conduction term was included in the usual boundary-layer equations for the flow. When the vertical conduction term was retained in the equations and wall temperatures of the form

$$T_w/T_\infty = 1 + \tau_0 x^n, \; x \geqslant 0, \; n > 1;$$

$$T_w/T_\infty = 1, \; x \leqslant 0$$

selected so that a thermal leading edge on the wall was assured, then the only solution available appeared to be an asymptotic solution in powers of $1/x^{(n+3)/2}$. This series converges rapidly to that which had been found in closed form for the region above the leading edge in which the vertical conduction term is not significant. This asymptotic solution did not, of course, allow an approach to the thermal leading edge and all attempts to find a solution for the leading edge region failed.

A preliminary exploration of the comparably simpler problem of heat conduction in a solid wedge having surface temperatures assigned to the natural convection case gave a clue that the form of the temperature distribution

$$T/T_\infty = 1 + \tau(x)\,(1 - y/\delta)^2$$

assumed for the treatment of the natural convection case may not be suitable at the leading

edge region and prevented an acceptable approach to it.

As a result, it was decided to start with a more generalized setting in the temperature and velocity distributions and make the necessary simplifications under guidance of the boundary conditions.

At this stage temperatures and velocities of the form

$$T/T_\infty = 1 + \tau + \tau_1 y + \tau_2 y^2 + \tau_3 y^3 + \tau_4 y^4 \tag{1}$$

$$U = u y + u_1 y^2 + u_2 y^3 + u_3 y^4 + u_4 y^5 \tag{2}$$

in which the τ's and u's were assumed functions of x alone, were taken.

The following boundary conditions were imposed:

For the temperature distribution on the wall, the form

$$T_w/T_\infty = (T/T_\infty)_{y=0} = 1 + \tau \equiv 1 + \tau_0 x^n, \quad n > 1 \tag{3}$$

in which the restriction $n > 1$ provides

$$(\mathrm{d}T_w/\mathrm{d}x)_{x=0} = 0$$

and hence assures no downward conduction near the wall at $x = 0$.

The velocity at the wall and the vertical velocity at the edge of the boundary layer must both be zero so that

$$U_{y=0} = U_{y=\delta} = 0. \tag{4}$$

There should be no vertical shearing stresses at or adjacent to the edge of the boundary layer, hence

$$(\partial U/\partial y)_{y=\delta} = (\partial^2 U/\partial y^2)_{y=\delta} = 0. \tag{5}$$

There should be no heat conduction at the edge of the boundary layer, hence

$$(\partial T/\partial x)_{y=\delta} = (\partial T/\partial y)_{y=\delta} = 0. \tag{6}$$

Finally at the wall and particularly near $x = 0$ the requirement of zero velocity leads to (7).

$$[\partial^2 T/\partial x^2 + \partial^2 T/\partial y^2]_{y=0} = 0. \tag{7}$$

Upon imposition of the above boundary conditions the equations (1) and (2) become

$$T/T_\infty = 1 + \tau + \tau_1 y - \tau'' y^2/2 - (4\tau + 3\tau_1 \delta - \tau'' \delta^2)(y/\delta)^3 + (3\tau + 2\tau_1 \delta - \tau'' \delta^2/2)(y/\delta)^4 \tag{8}$$

$$U = (1 - y/\delta)^3 [u\delta (y/\delta + y^2/\delta^2) + u_1 y^2] \tag{9}$$

which now contain only the four functions δ, τ_1, u and u_1.

It is evident that τ_1 is a wall heat-transfer function while u is the wall velocity shear function. It will be shown that u_1 relates to the magnitude and location of the peak velocity if it is selected so that a similarity solution for the velocity distribution is to result.

The equations (8) and (9) may now be used to reduce the boundary-layer equations for the leading edge region in integral form

$$-g \int_0^\delta (\rho_\infty - \rho)\,\mathrm{d}y + \frac{\mathrm{d}}{\mathrm{d}x} \int_0^\delta \rho U^2\,\mathrm{d}y + \mu (\partial U/\partial y)_{y=0} = 0 \tag{10}$$

$$c_p g \frac{\mathrm{d}}{\mathrm{d}x} \int_0^\delta \rho U (T - T_\infty)\,\mathrm{d}y + k \int_0^\delta (\partial^2 T/\partial x^2 + \partial^2 T/\mathrm{d}y^2)\,\mathrm{d}y = 0 \tag{11}$$

to ordinary differential equations. The resulting equations are nonlinear and of order one and two respectively. They are subject to further simplification by a transformation on the heat-transfer function τ_1 and, as indicated above, by the retention of similarity on the velocity distribution.

The transformation

$$\tau_1 = \mathrm{d}\bar{\tau}_1/\mathrm{d}x \tag{12}$$

reduces the energy equation to a first-order equation and the selection of the function u_1, such that

$$u_1 \delta = -c u, \quad 0 \leqslant c \leqslant 4 \tag{13}$$

provides similarity in the velocity distribution and the constant c provides a choice either of the peak value magnitude of the velocity distribution or in the location of this peak value in the

boundary-layer flow. Figure 1 shows velocity distributions for $c = 4$ and $c = 0$. Values of $c > 4$ would bring the peak closer to the wall but would introduce negative values of U close to the boundary-layer edge $y/\delta = 1$. The previous solutions for constant temperature wall sections

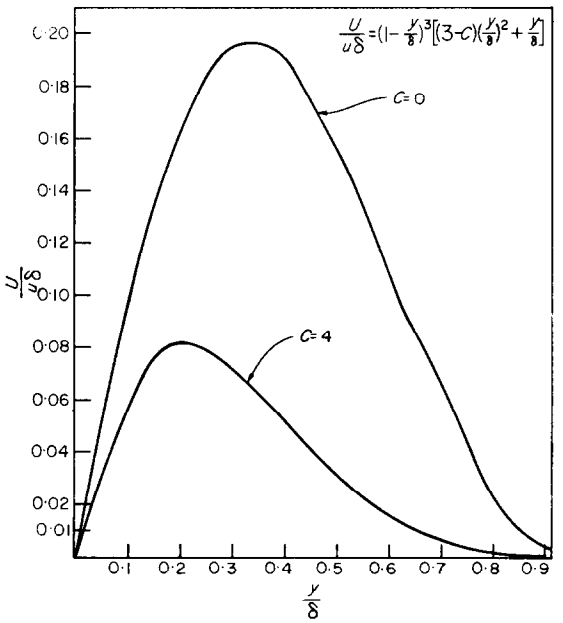

FIG. 1. Effect of parameter c on velocity distribution.

gave velocity distributions corresponding to $c = 0$ and a peak value at $(y/\delta)_{\text{peak}} = \frac{1}{3}$. Values of $c < 0$ should give peak value positions further from the wall then $y/\delta = \frac{1}{3}$ and even greater peak values then those for $c = 0$. Both of these results are considered unlikely in the leading edge region.

With the help of the qualifications discussed above, the equations 8 and 9 will take (10) and (11) into equations

$$k\left\{\frac{\mathrm{d}}{\mathrm{d}x}\left[3\tau\delta/5 + 3\bar{\tau}_1'\,\delta^2/20 - \tau''\,\delta^2/60\right]\right\} - \bar{\tau}_1 + \rho_\infty c_p g u \{A\,\tau''\,\delta^4 + B\,\tau\,\delta^2 + C\,\bar{\tau}_1'\,\delta^3\} = 0 \qquad (14)$$

$$-g\{3\tau\delta/5 + 3\bar{\tau}_1'\,\delta^2/20 - \tau''\,\delta^3/60\} + E\,\mathrm{d}(u^2\,\delta^3)/\mathrm{d}x + \nu u = 0 \qquad (15)$$

in which

$$A = c/36 - 11/72$$
$$B = -31c/36 + 11/2$$
$$C = -c/4 + 13/9$$
$$E = (6c^2 - 69c + 208)/13860.$$

Since these equations contain the three functions δ, u and $\bar{\tau}_1$ additional conditions must be found for a complete solution of the problem. These additional conditions are provided by the process of matching the leading edge solution with that above the leading edge region which is already available. The further conditions needed will be introduced later in the paper when the matching process is treated.

One verifies readily that equations (14) and (15) have a general solution of the form

$$\left.\begin{aligned}\delta &= \delta_0\,x^{r_3}[1 + \delta_1\,x^s + \delta_2\,x^{2s} + \ldots]\\ u &= U_0\,x^{r_2}[1 + U_1\,x^s + U_2\,x^{2s} + \ldots]\\ \tau_1 &= T_0\,x^{r_1}[1 + T_1\,x^s + T_2\,x^{2s} + \ldots]\end{aligned}\right\} \qquad (16)$$

in which the exponents r_1, r_2, r_3 and s are functions of n definable in part by the differential equations (14) and (15). One finds from the differential equations that for admissible families of solutions we must have

$$\left.\begin{aligned}r_1 &= n + r_3 - 2\\ r_2 &= n + r_3\\ s &= (n+3)/m\end{aligned}\right\} \qquad (17)$$

in which m is a positive integer. Additional physical qualifications are available to aid in the selection of the two independent parameters of equation (17). If the heat-transfer coefficient is to remain finite at $x = 0$ and since $n - 1 > 0$ it is clear from the first equation in (17) that $r_3 \geqslant 1$. It may further be shown that for $r_3 < 1$ the temperature distribution given in (8) will contain temperatures below ambient near the edge of the boundary layer in the neighborhood of the leading edge.

Deferred for the moment are arguments for the fact that there are reasonable qualifications which indicate that values $r_3 > 1$ are not suitable so that it appears that $r_3 = 1$ must be taken as

most suitable. Also deferred for the moment is a discussion about the selection of the parameter m.

When the expansions (16) are put into the differential equations (14) and (15) the first terms of the resulting expansions in powers of x depend respectively only on the conduction term of the energy equation and the buoyancy and viscous terms of the momentum equation. Thus, it appears that the fluid is acting as a relatively slow moving viscous fluid in which energy transfer is dominantly by conduction and the momentum transfer by buoyancy and viscous shear. These first terms referred to determine T_0 and U_0 to be

$$\left.\begin{aligned} T_0 &= \{\tau_0\,\delta_0\,[1 - n(n-1)\,\delta_0^2/36] \\ &\quad 3\,n(n+1)/5\}/[1 - 3\,n(n+1)\,\delta_0^2/20] \\ U_0 &= g\,\tau_0\,\delta_0\,[36 + 9\,T_0\,\delta_0/\tau_0 - n/n - 1) \\ &\quad \delta_0^2]/60\,\nu = g\,T_0/\nu\,n(n+1) \end{aligned}\right\} \quad (18)$$

These equations point up the startling and unanticipated result that in the thermal leading edge neighborhood the conduction of heat is into the wall rather than out of it as would have been expected.

THE REVERSE CONDUCTION AT THE LEADING EDGE

For the current wall temperature distribution under study ($T/T_\infty = 1 + \tau_0\,x^n$, $n > 1$, $\tau_0 > 0$) one must expect the convective velocities will always be positive (upward) and, hence, we need a solution in which $U_0 > 0$. It follows from the second of equations (18) that $T_0 > 0$ and, hence, in a small enough neighborhood of the leading edge the heat conduction will be into the wall. It is plausible that this phenomenon will occur in all leading edge cases where the wall temperature gradient is zero at the leading edge and positive immediately above it. For the particular case in hand this conclusion and equations (18) enable the determination of an admissible range for the leading edge slope parameter δ_0.

ADMISSIBLE RANGE FOR LEADING EDGE SLOPE

From equations (18) one finds readily that there are two δ_0 ranges which will give a positive T_0. They are

$$\left.\begin{aligned} \delta_0^2 &> 36/n(n-1) \\ \delta_0^2 &< 20/3n(n+1) \end{aligned}\right\} \quad (19)$$

and it may be shown that only the second of these admits temperature distributions which avoid values that include temperatures such that $T/T_\infty < 1$.

For this purpose we compute the temperature gradient from equation (8) in the form

$$\begin{aligned} \mathrm{d}(T/T_\infty)/\mathrm{d}(y/\delta) &= (1 - y/\delta)\,[\tau_1 \\ &\quad + (\tau_1 - \tau''\,\delta)\,(y/\delta) + (-12\,\tau/\delta - 8\,\tau_1 \\ &\quad + 2\,\tau''\,\delta)\,(y/\delta)^2] \equiv (1 - y/\delta)\,Q\,(y/\delta) \end{aligned} \quad (20)$$

and study the quadratic form $Q\,(y/\delta)$ in the neighborhood of the leading edge. For the selected value $r_3 = 1$ and in the neighborhood of the leading edge the quadratic form may be written

$$\begin{aligned} &n(n-1)\,\delta_0\,\tau_0\,x^{n-1}\,[p + (p-1)\,(y/\delta) \\ &\quad + (-1/3\,e^2 - 8\,p + 2)\,(y/\delta)^2] \end{aligned} \quad (21)$$

in which

$$\begin{aligned} p = T_0/\delta_0\,\tau_0\,n(n-1) &= (e^2 - 1)/9\,[e^2 \\ &\quad - 5\,(n-1)/27\,(n+1)] \\ \delta_0^2 &= 36\,e^2/n(n-1) \end{aligned}$$

Now for $e^2 > 1$ we have the first inequality of (19) and

$$\begin{aligned} 0 < p = (e^2 - 1)/9\,[e^2 &- 5\,(n-1)/27 \\ &(n+1)] < 1/9 \end{aligned} \quad (22)$$

so that

$$[Q\,(y/\delta)]_{y=0} = p > 0$$

$$[Q\,(y/\delta)]_{y=\delta} = Q\,(1) = 6\,p + 1 - 1/3\,e^2 > 0$$

and in the interval $0 \leqslant y/\delta \leqslant 1$ the form Q has either two real roots or no real roots. Two distinct roots would mean both a maximum and a minimum in T/T_∞ in $0 < y/\delta < 1$ and, hence, some acceptable T/T_∞ values less than one. A double root would mean a horizontal inflection point in the T/T_∞ distribution and hence the absence of the maximum which must be present. The absence of real roots also cannot be accepted

because the required maximum is not provided. It follows the δ_0 range defined by

$$\delta_0 > 36/n(n-1)$$

must be rejected. For

$$e^2 < 5(n-1)/27(n+1)$$

we have

$$1 - 1/3\, e^2 < 1 - 1/[(15)\,(n-1)/(n+1)\,27] = 1 - 9\,(n+1)/5\,(n-1) < 0$$

so that

$$\left.\begin{aligned} Q\,(0) &= p > 0 \\ Q\,(1) &= -6\,p + 1 - 1/3\, e^2 < 0 \end{aligned}\right\} \quad (23)$$

and the quadratic form $Q\,(y/\delta)$ has one and only one real root in $0 < y/\delta < 1$ which must correspond to a maximum in the distribution. Thus, it is clear that to assure upward convective velocities and temperatures such that $T/T_\infty \geqslant 1$ the δ_0 range of values must be limited to that defined by the second of the inequalities in (19).

Selection of family of solutions corresponding to $r_3 = 1$

As has been indicated a selection from two families of solutions is still to be made [see (17)]. These correspond to

$$r_3 = 1, \quad r_1 = n - 1, \quad r_2 = n + 1, \quad s = (n+3)/m \quad (24)$$

and

$$r_3 = 1 + (n+3)/m, \quad r_1 = (n-1) + (n+3)/m, \quad r_2 = (n+1) + (n+3)/m, \quad s = (n+3)/m \quad (25)$$

in which m is a positive integer.

The second family ($r_3 > 1$) is rejected for two reasons. First, this family yields solutions with the boundary-layer edge tangent to the wall at the leading edge so that the isotherms coming out of the wall in that region would have to make extremely abrupt and sharp turns which would make for questionable physical validity. The family for $r_3 = 1$ allows more space for the isotherm turn. Secondly, on the basis of past experiments one must expect that the wall temperature gradient should become negative fairly rapidly as one moves up away from the leading edge and its numerical value should change fairly rapidly to values experienced with natural convections above the leading edge. Some preliminary calculations which compare the rate of change of the wall gradients $\partial T/\partial y$ as x increases from zero indicate that the family for $r_3 = 1$ gave the more rapid changes to the negative values needed.

For the reasons above the family defined by $r_3 = 1$ was selected for solution of the leading edge problem.

Selection of the parameter s

One finds on the substitution of (16) in (14) and (15) to compute the coefficients $\delta_0, \delta_1, \ldots$; $U_0, U_1, U_2, \ldots$; $T_0, T_1, T_2, \ldots$ that the first few terms of each of these sequences are independent of the convective terms in both the energy and momentum equations. Further, that the number of the terms independent of the convective phenomena depends on the value of s or indirectly on the choice of m. For $m = 1$ only the first terms are independent of the convective effects but $s > 4$ and it becomes necessary to cope with abrupt changes in the dependent variables when x approaches some critical value above the leading edge such as the point of conduction reversal on the wall. Since it is desirable to get past such a position with the leading edge solution, abrupt changes of this character are to be avoided by the selection of s as close to 1 as is feasible, It may be shown that m may be selected so that $1 \leqslant s \leqslant 5/4$ for all $n > 1$. For this range of s values we will have $m \geqslant 4$ so that the convective effects do not influence the coefficients of (16) before the fourth terms and this suggested that the equations (14) and (15) might be further approximated by dropping the convective terms. Physically this means that the transport of energy is essentially by heat conduction and the motion is that of a slow moving viscous flow.

With the last approximation the leading edge boundary-layer equations may be written

$$3\,\tau\delta/5 + 3\,\tau_1\,\delta^2/20 - \tau''\,\delta^3/60 - \int_0^x \int_0^x \tau_1\,(\mathrm{d}x)^2 = 0 \quad (26)$$

$$-g\,(3\,\tau\delta/5 + 3\,\tau_1\,\delta^2/20 - \tau''\,\delta^3/60) + \nu\,u = 0. \quad (27)$$

Solution of the simplified system

These equations have a simple solution in closed form if the function τ_1 is restricted to two terms of its expansion shown in equation (16). It will be assumed to have the form

$$\tau_1 = \bar{T}_0 \, x^{n-1} \, (x_1^s - x^s) \qquad (28)$$

in which x_1 is the position of the expected conduction reversal on the wall and $\bar{T}_0 > 0$ so that the heat conduction is from the wall to the fluid for positions $x > x_1$.

With the selected form of the function τ_1, equation (26) has a solution

$$X^s = (k_1 - D^2)/(1 - D^2) - k_2 \, D \, (k_3 - D^3)/P \, (1 - D^2) \qquad (29)$$

in which

$$D = \bar{\delta}/KX, \quad \bar{\delta} \equiv \delta/x_1, \quad K^2 = 20/3 \, (n + s) \, (n + s + 1)$$

$$X = x/x_1$$

$$k_1 = (n + s) \, (n + s + 1)/n \, (n + 1)$$

$$k_2 = n \, (n - 1) \, K/9$$

$$k_3 = 27 \, (n + s) \, (n + s + 1)/5 \, n(n - 1)$$

$$P = \bar{T}_0 \, x_1^s/\tau_0$$

and in which the parameter P turns out to be very interesting and significant. The value $P = P_{cr} \equiv k_2(k_3 - 1)/(k_1 - 1)$ divides the solutions into two classes corresponding to $P > P_{cr}$ and $P < P_{cr}$. For $P > P_{cr}$ (29) gives an X, $\bar{\delta}$ system of curves of the type shown in Fig. 2. Neither leg of the triangular section is suitable for the boundary-layer edge function δ. The one steeper to the wall gives the high δ_0 values which were rejected because the temperature distribution for such cases contained values $T/T_\infty < 1$. The shallower one has the wrong curvature at the top for the matching process needed for a complete solution. One would also find that the shallower leg gives relatively inadequate temperature gradients near the wall for the matching process. For $P = P_{cr}$ the two branches of the system merge into a single branch as shown in Fig. 3. This result is also unsuitable because of the steepness of the leg emerging at $X = 0$ and because the turn where matching must occur is for values of $X < 1$. Matching of solutions is

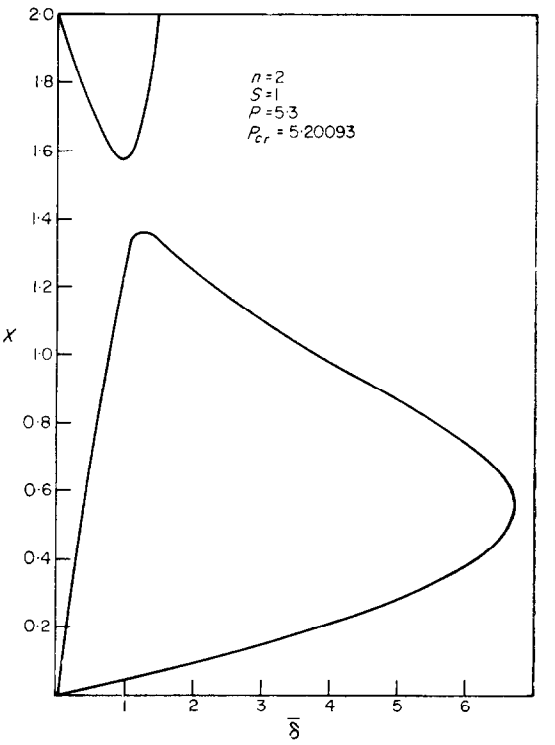

FIG. 2. Thickness distribution solution when $P < P_{cr}$.

expected at $X > 1$, that is, above the conduction reversal point. For $P < P_{cr}$ one gets curves of the type shown in Fig. 4. The leading edge slope δ_0 is clearly less than one and, hence, satisfies the criteria $\delta_0^2 < 20/3n(n + 1) = 10/9$, $n = 2$ developed from the study of the inequalities (19). Also these curves have the proper curvature for matching at some $X > 1$. It thus appears that admissible solutions are available for values of $P < P_{cr}$.

Selection of the parameter P

A value of P is sought which will most suitably take the temperature distribution of the leading edge solution into temperature distributions needed for matching with the solutions above the leading edge. The temperature distribution used in reference 1 for wall temperatures of the type $T_w/T_\infty = 1 + \tau_0 \, x^n$ took a form

$$T/T_\infty = 1 + \tau_0 \, x^n \, (1 - y/\delta)^2 \qquad (30)$$

which has plausibility from the very limited

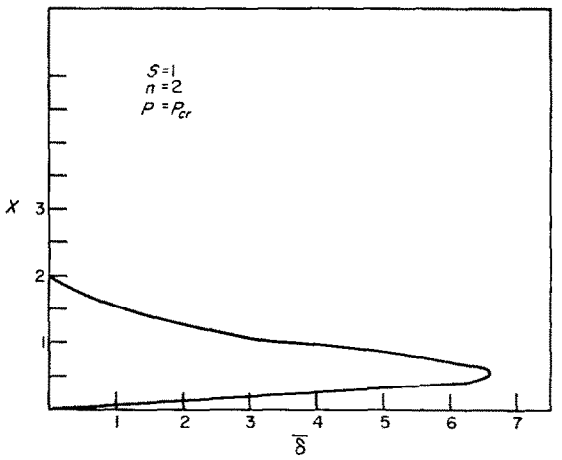

FIG. 3. Thickness distribution solution when $P = P_{cr}$.

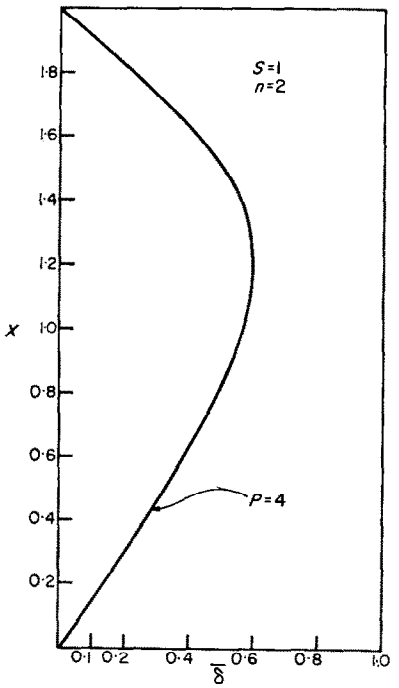

FIG. 4. Thickness distribution solution when $P < P_{cr}$.

experimental data showing a parabolic temperature distribution. For the present purpose this form will be generalized to

$$T/T_\infty = 1 + \tau_0 x^n (1 - y/\delta)^{s_1} \qquad (31)$$

which should remain a plausible form so long as s_1 does not deviate greatly the value 2. This new form is introduced for the purpose of providing an additional parameter to enable a smoother transition of the solutions at the matching position. If one introduces the temperature variable

$$\bar{T} \equiv [T/T_\infty - 1]/\tau$$

then

$$\bar{T} = (1 - y/\delta)^{s_1}$$

and the normal wall temperature gradient $G_{\bar{T}}$ may be written

$$G_{\bar{T}} = -s_1 \qquad (32)$$

and this will be one of the boundary conditions for solution-matching. Since the gradient should have the same value at the matching position in both solutions and since s_1 should not deviate greatly from the value 2, we must seek a P in the leading edge solution which yields a gradient $G_{\bar{T}}$ as close to 2 as is available. It turns out that available gradient values are all less than 2 and that they increase with P as P approaches P_{cr}. Thus, the closest $G_{\bar{T}}$ value to 2 is obtained by letting $P \to P_{cr}$. Figures 4, 5 and 6 show the boundary-layer thickness distribution for $n = 2$ as P increases toward $P_{cr} = 5{\cdot}2009$. The leg emerging from the leading edge has become quite linear and the turning section at which matching is expected has sharpened considerably. In Fig. 6 the P value is quite close to P_{cr} and the turn is such that the matching position is essentially determined. Also note that $G_{\bar{T}}$, which is negative above $X = 1$ (the reverse conduction position), has a numerical value close to 1·8 at the matching position and also that it has an essentially rapid linear numerical growth toward the peak value.

Location of matching position

It was observed in the numerical work for determining thickness distributions when P was close to P_{cr} (see Figs. 5 and 6) that the usable parts of the functions defined by equation (29) (that is, the essentially linear part emerging from the leading edge $X = 0$) corresponded to values of D which were quite close to unity. Thus, we may put

$$\left.\begin{aligned} 1 - D &= \epsilon/r, \quad r = 0(\epsilon) \\ P &= P_{cr}(1 - \epsilon) \end{aligned}\right\} \qquad (33)$$

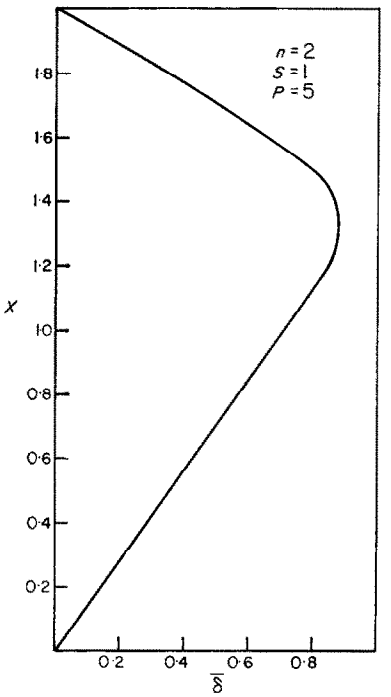

FIG. 5. Thickness distribution solution $P = 5 < P_{cr}$.

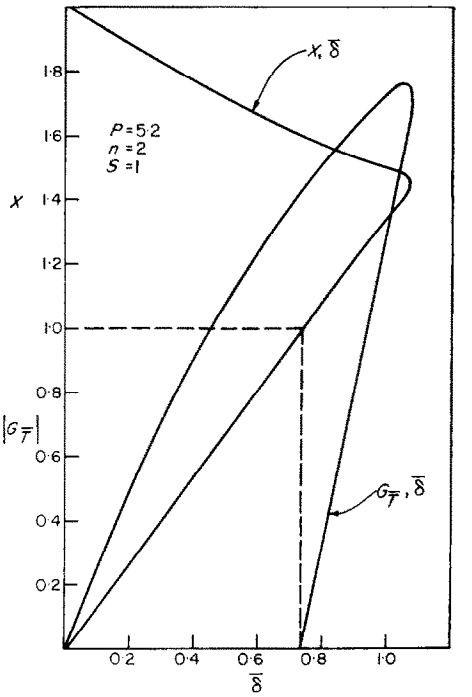

FIG. 6. Thickness distribution and wall temperature gradient when $P = 5{\cdot}2 < P_{cr}$.

and approximate equation (29) by

$$X^s = 1 - (k_1 - 1)/(k_3 - 1) + (k_1 - 1)(1 - r)/2 \qquad (34)$$

The values of X near the sharp turn position will correspond to small values of r so that we may estimate the X matching position by

$$X^s_{\text{mat}} = \{1 + [(n+s)(n+s+1)/n(n+1) - 1]/2 - [(n+s)(n+s+1)/n(n+1) - 1]/[5{\cdot}4(n+s)(n+s+1)/n(n-1) - 1]\} \qquad (35)$$

Thickness distribution to the point of matching

Since, as has been indicated, the values of D from the leading edge to the position of matching are close to unity we have from (30)

$$\bar{\delta} = KXD \sim KX = \sqrt{[20/3(n+s)(n+s+1)]}\,X = \delta_0 X \qquad (36)$$

The thickness at the matching position will be $\bar{\delta}_{\text{mat}} = \delta_0 X_{\text{mat}}$.

Wall temperature gradient at the matching position

We have from (8) and (35)

$$\left.\begin{aligned} G_{\bar{T}} &= \tau_1\,\delta/\tau = \bar{T}_0\,x_1^s\,x^{n-1}(1 - x^s)\,x\,DK/\tau_0\,x^n = PKD(1 - x^s) \\ (G_{\bar{T}})_{\text{mat}} &= -2 + 10\,n(n-1)/9\,(n+s)(n+s+1) \end{aligned}\right\} \qquad (37)$$

and it is seen that for n close to 1 the gradient will be quite close to the -2 used in reference 1. Further, the value of s_1 of equation (32) may now be determined as

$$s_1 = 2 - 10\,n(n-1)/9\,(n+s)(n+s+1) \qquad (38)$$

in order to match temperature gradients of the leading edge solution with the usual solution above this position.

As a matter of passing interest and to disclose additional geometric significance of some of the parameters it may be shown that the slope of the isotherms entering the wall in the leading edge region may be written

$$(\mathrm{d}y/\mathrm{d}x)_{y=0}^{\text{isotherm}} = -\tau'/\tau_1 = -n/P_{cr}\,(1 - x^s) \tag{39}$$

The position of reverse conduction

Equation (35) predicts the nondimensional matching position in terms of the position x_1 of reverse conduction. We may determine the matching position as a function of known parameters and thus also find the reverse conduction position in terms of these parameters. For this purpose and to optimize a matching of the velocities at the matching position we return to the problem above the leading edge and generalize the velocity form used in that problem in addition to the generalized temperature form introduced by equation (32).

We write

$$U = n\,(y/\delta)\,(1 - y/\delta)^{s_2} \tag{40}$$

For $s_2 = 2$ this becomes the form used in reference 1. If one drops the vertical conduction term in equation (11) and assumes the temperature form (32) and the velocity form (40) then (10) and (11) may be reduced to the ordinary equations

$$\left.\begin{aligned} r'\,u\,\delta^2 &= \tau(u'\,\delta^2 + u\,\delta\delta' - c_2) = 0 \\ 2\,uu'\,\delta^2 &+ u^2\,\delta\delta' - c_3\,\tau\,\delta^2 + c_4\,u = 0 \end{aligned}\right\} \tag{41}$$

in which

$$c_2 = s_1\,(s_1 + s_2 + 1)\,(s_1 + s_2 + 2)\,\nu/Pr$$

$$c_3 = (2\,s_2 + 1)\,(2\,s_2 + 2)\,(2\,s_2 + 3)\,g/2\,(s_1 + 1)$$

$$c_4 = (2\,s_2 + 1)\,(2\,s_2 + 2)\,(2\,s_2 + 3)\,\nu/2$$

The equations (41) have the following closed form solution with appropriate starting values at some starting X above the leading edge.

$$\left.\begin{aligned} u &= 2\,\tau_0^{1/2}\,x^{(1+n)/2}\,\sqrt{\{c_3/[5 + 3\,n + c_4\,(3 + 5n)/c_2]\}} \\ \delta &= 2\,x^{(1-n)/4}\,\sqrt{[c_2/(3 + 5\,n)]/\{4\,\tau_0\,c_3/[(5 + 3\,n) + c_4\,(3 + 5\,n)/c_2]\}^{1/4}} \end{aligned}\right\} \tag{42}$$

Now since the δ's of both solutions must be equal at the matching position it follows from (36) and (42) that

$$x_{\text{mat}}^{(n+3)/4} = \sqrt{\left[\frac{3\,(n + s)\,(n + s + 1)\,c_2}{5\,(3 + 5n)}\right]\Big/ \{4\,\tau_0\,c_3/[5 + 3\,n + c_4\,(3 + 5\,n)/c_2]\}^{1/4}} \tag{43}$$

and this combined with equation 35 for X_{mat} determines the conduction reversal position as a function of n, τ_0, P_{cr}, s_2 and c. There remains a determination of the parameters s_2 and c.

Determination of velocity parameter s_2 and c

Because of the approximation methods used, a precise matching of the temperature and velocity distributions at the matching position for the two solutions involved cannot be anticipated. Approximate matching is available and the matching process itself enables a complete determination of all the parameter variables of the solutions. Precise matching of the wall temperature gradients has provided a determination of s_1. Values of c and s_2 may be determined by a matching of the peak velocities and the positions of these peak velocities.

It may be shown readily that the upper solution has a peak velocity

$$(U_{\max})_{\text{US}} = u\,s_2^{s_2}/(1 + s_2)^{(1+s_2)} \tag{44}$$

at the position

$$(y/\delta)_{\substack{\text{US} \\ \max}} = 1/(1 + s_2) \tag{45}$$

Correspondingly the $(U_{\max})_{\text{LES}}$ may be written

$$(U_{\max})_{\text{LES}} = u\,\delta\{[1 - (y/\delta)_{\max}]^3\,[(3 - c)\,(y/\delta)_{\max}^2 + (y/\delta)_{\max}]\} \tag{46}$$

in which

$$(y/\delta)_{\substack{\text{LES} \\ \max}} = 1 - \frac{2\,(7 - 2\,c) - \sqrt{[(7 - 2\,c)^2 - 15\,(4 - c)\,(3 - c)]}}{5\,(3 - c)} \tag{47}$$

A direct algebraic relationship between s_2 and c for equal values of maximum velocities is evidently not available from these equations so that graphical methods were employed.

Let K_{s_2} be a function of s_2 such that

$$U_{\max,\,\mathrm{mat}} = u_0\, x_{\mathrm{mat}}^{(1+n)/2}\, s_2^{s_2}/(1+s_2)^{(1+s_2)} = K_{s_2}\,\frac{P_{cr}\,\tau_0\,g}{n\,(n+1)}\cdot x_{\mathrm{mat}}^{n+1}\left\{1-\frac{n(n+1)\,X^s}{(n+s)\,(n+s+1)}\right.$$

$$\left.\sqrt{[2/3\,(n+s)\,(n+s+1)]}\,x_{\mathrm{mat}}\right\} \tag{48}$$

and this determines a K_{s_2} in a form reducible to

$$K_{s_2} = \frac{18\,Pr\,FF_2\,(n+s)\,(n+s+1)\,(3+5n)}{[(5+3\,n)+(s_1+1)\,Pr\,F_2\,(3+5\,n)]\,[5{\cdot}4\,(n+s)\,(n+s+1)+n\,(n-1)]} \tag{49}$$

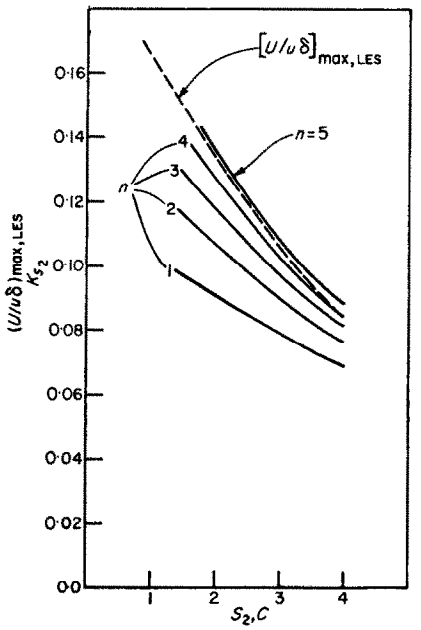

FIG. 7. Auxiliary curves for maximum velocity matching.

in which

$$F_2 = (2\,s_2+1)\,(2\,s_2+2)\,(2\,s_2+3)/2\,s_1\,(s_1+1)\,(s_1+s_2+1)\,(s_1+s_2+2)$$

$$F = s_2^{s_2}/(1+s_2)^{(1+s_2)}$$

This function has been plotted in Fig. 7 as a function of s_2 for values of $n = 1, 2, 3, 4$ and 5 together with the function $(U_{\max}/u\delta)_{\mathrm{LES}}$ of the parameter c [equations (46), (47)].

One obtains by cross plotting from Fig. 7 for fixed values of n and equal values of K_{s_2} and $(U/u\delta)_{\max}$ the family of curves Fig. 8, for

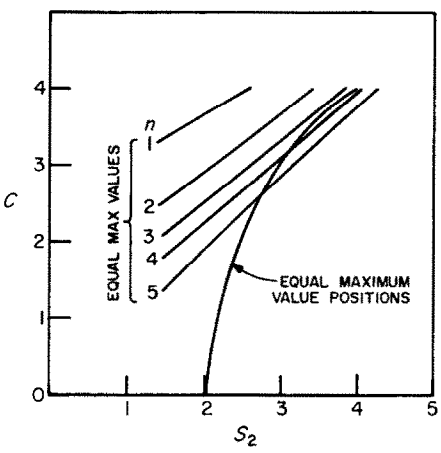

FIG. 8. Curves for equal maximum matching velocities and equal maximum value y positions.

values of c and s_2 giving equal maximum velocities at fixed values of n. Figure 8 also contains a plot of values of c and s_2 which provide the same positions of maximum velocity at the matching position of the solutions. The intersection of the latter with the equal maximum value family thus provides values of c and s_2 for equal maximum velocity values as well as the same positions for these values. It appears that such intersections will be available only for values of n greater than some number somewhat larger than 3. On the other hand, it is clear from Figs. 9 and 10 which compare matching velocity distributions for $c = 4$ and the corresponding s_2 taken from the equal maximum velocity curves (Fig. 8), that the lack of matching for positions of maximum velocity does not appear particularly significant except possibly for values of n near one. In the latter case the velocities in the

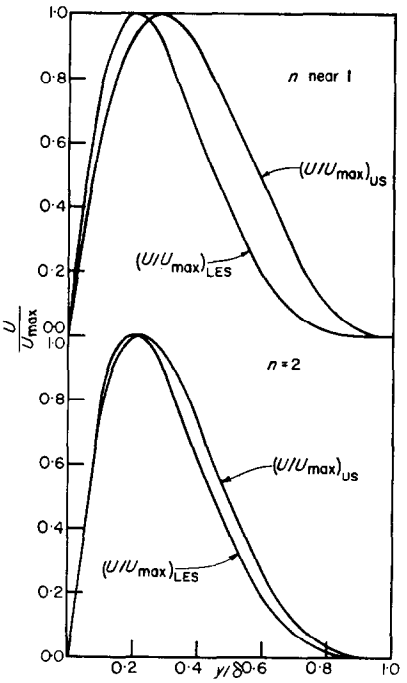

FIG. 9. Comparison of velocity distribution at matching position.

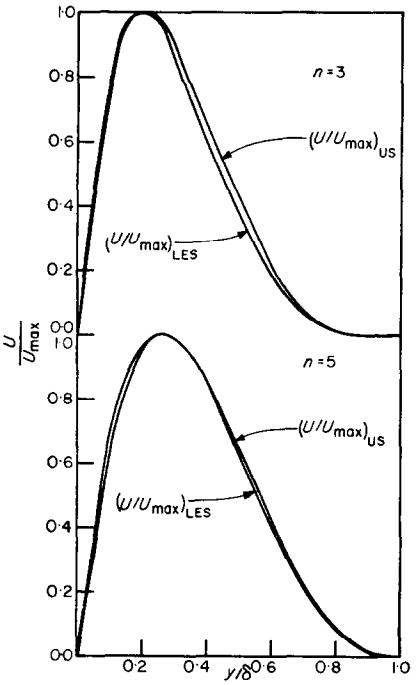

FIG. 10. Comparison of velocity distribution at matching position.

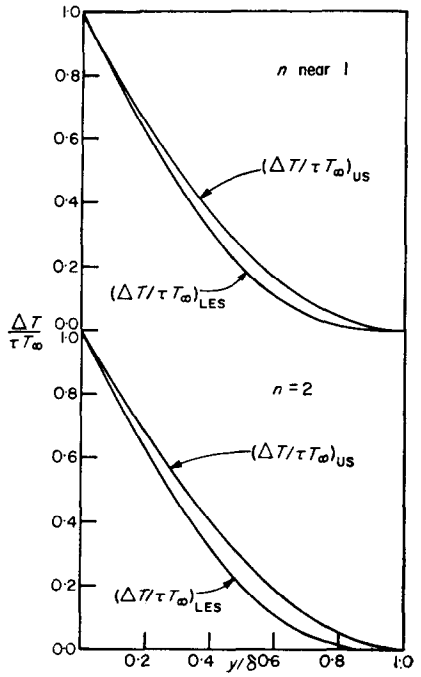

FIG. 11. Comparison of temperature distributions at matching position.

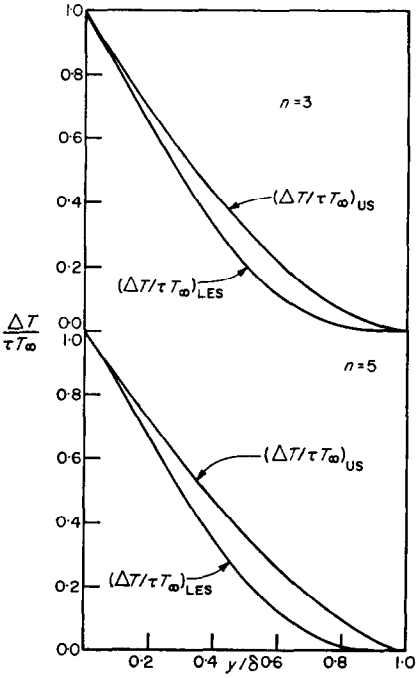

FIG. 12. Comparison of temperature distribution at matching point.

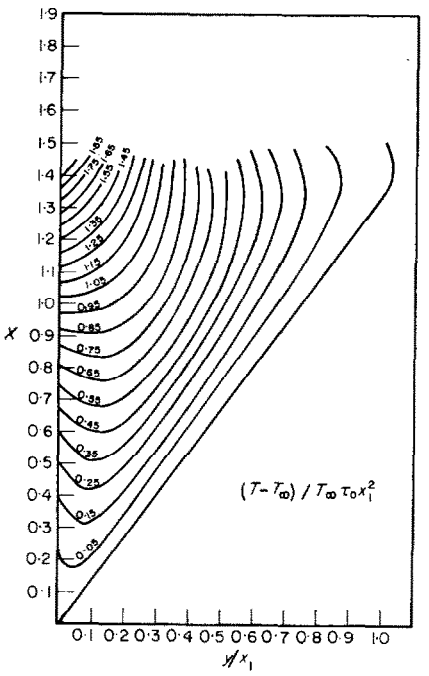

FIG. 13. Isotherms for constant temperature values $(T - T_\infty)/T_\infty\,\tau_0\,x_1{}^n$, $n = 2$.

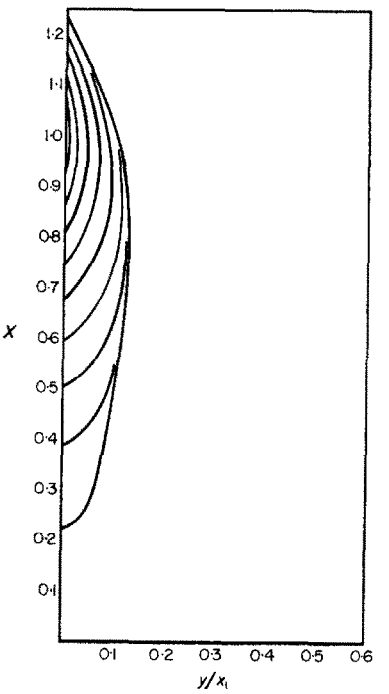

FIG. 14. Lines of heat conduction when $n = 2$.

outer part of the boundary layer could stand improved matching and the wall shearing stresses could stand better matching. It is probable that the matching in this instance could be improved by relaxing the other boundary matching requirements that have been set, such as wall heat transfer, maximum velocities and boundary layer thickness. Since values of n near one involve essentially a discontinuous vertical wall temperature gradient at the thermal leading edge actual physical settings of this kind are unlikely to occur and, hence, the value of working up improved matching characteristics for such values of n is very questionable, and thus was not attempted in this paper.

Comparison of wall shearing stresses at matching position

It may be shown that the wall shearing stresses of the solutions involved are respectively

$$\left.\begin{aligned}[(\partial U/\partial y)_{y=0}]_{\text{LES}} &= (u)_{\text{LES}} \\ [(\partial U/\partial y)_{y=0}]_{\text{US}} &= (u/\delta)_{\text{US}}\end{aligned}\right\} \quad (50)$$

These are each multiples of the function $\tau_0^{2/(n+3)}$ and thus a direct comparison of the wall stress at the matching position is available for variations in n. Table 1 makes the comparisons for the n range $1 < n \geqslant 5$.

Figures 11 and 12 compare temperature matching distributions for several values of n. In this instance it appears that the matching is best for the lower values of n which is contrary to what was found for the velocity matching. In any case the temperatures are reasonably well matched.

Isotherm and line conduction structure for the case $n = 2$

Figure 13 shows the isotherm structure from the leading edge to matching position when $n = 2$. The isotherms were obtained from the derived equations

$$\begin{aligned}(T - T_\infty)/T_\infty\,\tau_0\,x_1^n = X^n\,\{1 &+ P_{cr}\,K\,(1 \\ &- X)\,(y/\delta) - n\,(n-1)\,K^2\,(y/\delta)^2/2 - [4 \\ &+ 3\,P_{cr}\,K\,(1-X) - n\,(n-1)\,K^2]\,(y/\delta)^3 \\ &+ [3 + 2\,P_{cr}\,K\,(1-X) - n\,(n-1) \\ &K^2/2]\,(y/\delta)^4;\ y/x_1 = (y/\delta)\,KX. \end{aligned} \quad (51)$$

Table 1

n	Near 1	2	3	4	5
$[u/\tau_0^{2/(n+3)}]_{LES}$	25	5·96	2·47	1·24	0·73
$[u/\delta\,\tau_0^{2/(n+3)}]_{US}$	18	5·35	2·43	1·25	0·73

The heat conduction lines shown in Fig. 14 were determined analytically as the orthogonal trajectories of these isotherms.

It is evident thus that the present treatment of the thermal leading edge problem for wall temperatures of the form $T_w/T = 1 + \tau_0 x^n$ gives good quantitative matching results for values of $n \geqslant 2$ and qualitatively acceptable results even for values of n near one where the vertical wall temperature gradient (at $x = 0$) is essentially discontinuous. An experimental program is in process to test these results for the case $n = 2$. The reversed conduction effect has been confirmed.

REFERENCES

1. M. G. SCHERBERG, Natural convection near and above thermal leading edges on vertical walls, *Int. J. Heat Mass Transfer* **5**, 1001–1010 (1962).
2. M. G. SCHERBERG, Natural convection from wall sections of arbitrary temperature distribution by an integral method, *Int. J. Heat Mass Transfer* **7**, 501–516 (1964).

Résumé—La convection naturelle à partir d'une région de bord d'attaque thermique ($T_w/T_\infty = 1 + \tau_0 x^n, n > 1$) est déterminée et raccordée à la solution connue immédiatement au-dessus de cette région. On montre que, dans cette région, la conduction de la chaleur s'effectue vers le bas près de la paroi et s'écoule vers cette paroi juste au-dessus du bord d'attaque de telle façon qu'il y a une région juste au-dessus de ce point dans laquelle le transport de chaleur a une direction contraire à celle que l'on attendait. Des comparaisons des distributions de température et de vitesse à l'endroit de jonction des solutions sont données pour plusieurs valeurs de l'exposant n.

Zusammenfassung—Für einen Bereich am Beginn der thermischen Grenzschicht ($T_w/T_\infty = 1 + \tau_0 \cdot x^n, n > 1$) wird die freie Konvektion bestimmt und an die bekannte Lösung unmittelbar über diesem Bereich angeglichen. Es wird gezeigt, dass in diesem Bereich in Wandnähe Wärme mach unten geleitet wird, die kurz über der Entstehungsstelle der thermischen Grenzschicht in die Wand zurückströmt, so dass es gerade über diesem Punkt einen Bereich gibt, in welchem der Wärmeübergang der erwarteten Wärmestromrichtung entgegengesetzt ist. Für mehrere Werte des Exponenten n werden Vergleiche für Temperatur- und Geschwindigkeitsverteilungen an der Angleichstelle der Lösungen angegeben.

Аннотация—Получено решение для естественной конвекции для вертикальной стенки в области тепловой передней кромки ($T_w/T_\infty = 1 + \tau_0 x^n, n > 1$), которое смыкается с известным решением для области, лежащей непосредственно за ней. Показано, что в этом месте имеет место кондуктивная передача тепла вниз по потоку вблизи стенки, которое возвращается в стенку в месте, расположенном непосредственно за передней кромкой. Таким образом, имеется область над этой кромкой, где направление теплообмена противоположно ожидаемому направлению теплового потока. Для некоторых значений экспоненты "n" приводятся распределения температур и скоростей в окрестности смыканий решений.